Microcellular PVC

V. KUMAR, J. E. WELLER, AND R. MONTECILLO
University of Washington
Department of Mechanical Engineering
Seattle, Washington 98195, U.S.A.

1.0 INTRODUCTION

Very homogeneous microcellular foams, with average cell size of the order of 10 μm can be produced in PVC in a two stage process. In the first stage, a PVC sample absorbs carbon dioxide in a pressure vessel, maintained at 4.8 MPa (700 psi) and room temperature. In the second stage, the saturated sample is removed from the mold and heated to the glass transition temperature, causing cell nucleation and growth. The saturated samples may be heated to a temperature higher than the glass transition temperature to produce foams of lower density. Such a process was first conceived around 1980 by Suh [1] as a means to reduce the amount of plastics used in mass produced items. The basic process to produce microcellular plastics is discussed by Martini, Suh, and Waldman [2], who used nitrogen to create a microcellular structure in polystyrene. The bubble nucleation, growth, and processing issues in the polystyrene - nitrogen system have been studied by a number of investigators [3-8]. Recently, Kumar and coworkers have reported results on microcellular polycarbonate [9-11].

Figure 1 shows a schematic of the process to produce microcellular PVC. The process uses carbon dioxide which was chosen because of its high solubility in PVC [12,13], and thus the potential to produce a high cell nucleation density. A scanning electron micrograph of microcellular PVC is shown in Figure 2. The micrograph shows a very uniform nucleation of bubbles across the sample thickness. The left edge in Figure 2 shows a skin region with no bubbles that is approximately 25 μm in thickness. The thickness of this skin region can be controlled by allowing the carbon dioxide escape from the saturated sample surfaces for a predetermined length of time prior to heating [14]. The small cell size and high cell density in microcellular foams provide the possibility to foam thin wall parts in the 0.5 to 2 mm range, which can not be produced with conventional processes since the fewer and larger cells produced by these processes cause an excessive loss of strength. Additionally, in contrast to microcellular foams, structural PVC foams are typically characterized by a large variation in foam density across the foam thickness [15].

In this paper, we describe the process to produce microcellular PVC, and present experimental results on the relationship between some of the key process parameters.

2.0 EXPERIMENTAL

A rigid , transparent PVC formulation provided by the BFGoodrich Company in the form of molded sheets with an approximate thickness of 2 mm and a glass transition temperature of 78.2 °C was used. The density of PVC was measured to be 1.33 g/cm^3. The sheets were cut into 3 cm x 3 cm squares and placed in a pressure vessel connected to a CO_2 cylinder. The samples were then saturated with CO_2 gas at 4.8 MPa (700 psi) and 20 °C. During saturation, the samples were periodically removed from the pressure vessel and weighed on a precision balance with an accuracy of 10 μg. Because the amount of gas absorbed by the samples was on the order of 10 mg, this method of monitoring gas sorption provided sufficient accuracy. Upon saturation, the samples were removed from the pressure vessel and immediately foamed. The samples in this experiment were foamed in a glycerin bath maintained at the desired foaming temperature for a predetermined length of time. The temperature used to foam the sample, and the amount of time the sample is held at this temperature will be referred to as the foaming temperature and foaming time respectively. After foaming, the samples were placed in liquid nitrogen and fractured. The fractured surface, exposing the internal microstructure, was made conductive by deposition of Au-Pd vapor, and then the samples were studied using scanning electron microscopy (SEM). From the micrographs, the cell nucleation density and the average cell size were estimated using procedures described previously [9]. The cell density reported in this paper is the number of bubbles nucleated per cm^3 of the original, unfoamed polymer.

3.0 RESULTS AND DISCUSSION

3.1 SORPTION OF CO_2 IN PVC AND ITS EFFECT ON THE GLASS TRANSITION

Figure 3 shows a plot of the CO_2 uptake in mg CO_2 per g of polymer as a function of time for a saturation pressure of 4.8 MPa (700 psi). We see that the concentration at equilibrium reaches approximately 75 mg CO_2/g of PVC, or 7.5% by weight. Because of this high CO_2 concentration, we would expect significant plasticization of the polymer to occur, resulting in a lower glass transition temperature. A theoretical model has been developed to predict the glass transition in polymer - diluent systems by Chow [16], and has been shown to be in good agreement with experimental data [17]. According to this model, the glass transition temperature is given by

$$\ln\left(\frac{T_g}{T_{go}}\right) = \beta\left[(1-\theta)\ln(1-\theta) + \theta\ln(\theta)\right], \tag{1}$$

where

$$\beta = \frac{z\,R}{M_p\,\Delta C_{pp}} \tag{2}$$

$$\theta = \frac{M_p}{z\,M_d}\,\frac{\omega}{1-\omega} \tag{3}$$

ω = mass fraction of diluent,
M_p = molecular weight of the monomer,
M_d = molecular weight of the diluent,
R = gas constant,
T_{go} = glass transition of the pure polymer,
T_g^* = reduced glass transition,
z = coordination number,
ΔC_{pp} = excess transition isobaric specific heat of the polymer.

For PVC, Chiou et al. [17] suggests a ΔC_{pp} = 0.0693 cal/g °C. The glass transition of the pure PVC formulation used in this experiment was 78.2 °C. In

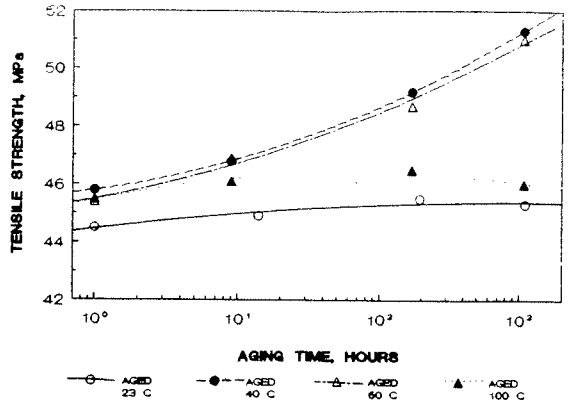

Figure 7. TENSILE STRENGTH OF AGED VINYL.

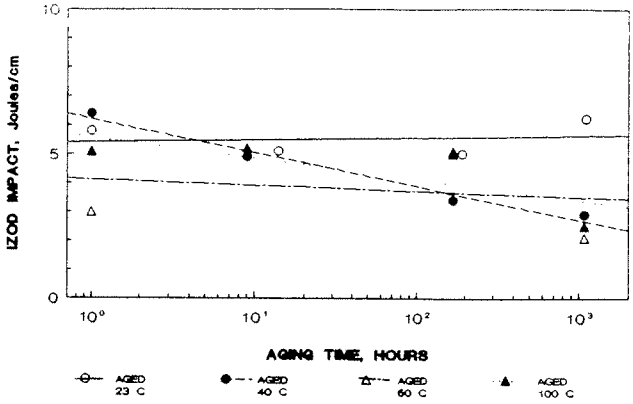

Figure 9. IZOD IMPACT OF AGED VINYL.

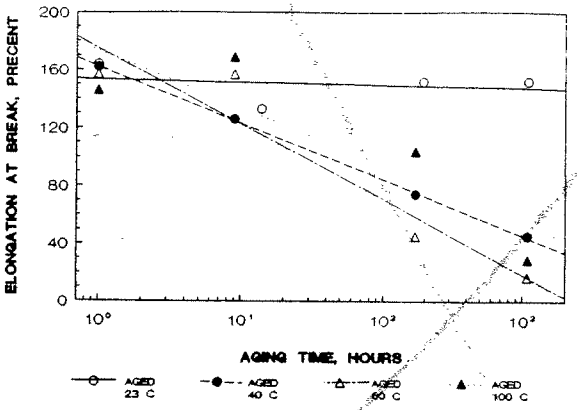

Figure 8. ELONGATION AT BREAK OF AGED VINYL.

addition, Chow [16] recommends a value of z = 2, based on comparison with experimental data. From Figure 3 we can see that at equilibrium, the concentration of CO_2 is approximately 75 mg/g, thus $\omega = 0.075$. Using the above values, the predicted Tg of PVC, saturated with a CO_2 concentration of 75mg/g is approximately 14 °C. The original microcellular process heated supersaturated sheets to the glass transition of the original material, as indicated in Figure 1. However, in light of the depression of the glass transition at high CO_2 concentrations, we expected bubbles to nucleate at temperatures significantly below the T_g of the original material.

3.2 EFFECT OF TEMPERATURE ON CELL NUCLEATION AND GROWTH

We investigated the effect of foaming temperature on cell nucleation and growth by foaming samples for 30 seconds at subsequently higher temperatures. When a sample is heated, foaming becomes evident as the sample turns white. This visual observation of bubble nucleation and growth was possible since we were using a clear, transparent formulation of PVC. As the bubbles grow to a size where light can be diffracted, the sample begins to look white and becomes opaque. The samples foamed at 40, 45, and 50 °C did not 'turn white,' and were therefore considered to not have foamed in our context. The first visible foam was produced at 55 °C. Samples were then foamed at 5 °C intervals up to a temperature of 120 °C. This broad range of temperatures was employed to investigate the effect of foaming temperature on the foam microstructure and the resulting foam density. Figure 4 shows a photograph of SEM micrographs of PVC foamed at increasing temperatures. All micrographs were taken at a magnification of 1000X in order to allow a visual evaluation of the effect of foaming temperature on the microstructure. As expected, we can see that nucleation has occurred at temperatures significantly below the original glass transition temperature, and that a microcellular structure can be achieved within the range of foaming temperatures explored. We can also see that the number of bubbles in the micrograph is increasing with temperature, implying that the nucleation density is increasing with increasing foaming temperature. Somewhat surprisingly, we note that the average cell diameter remains fairly constant over the range of foaming temperatures. Figure 5 is a plot of the cell nucleation density as a function of the foaming temperature. Note that the cell density in number of cells per cm^3 of original polymer has been plotted on a log scale. From Figure 5 we can see that the nucleation densities are of the order 10^7 - 10^9 cells/cm^3 in the range of foaming temperatures explored. Furthermore, we can see that nucleation in PVC shows an Arrhenius behavior within this foaming temperature. The data of Figure 5 is replotted in Figure 6, as a function of reciprocal temperature. From a least squares fit of the data on this plot, the activation energy associated with cell nucleation was determined to be 63.92 kJ/mol.

The average cell diameter is plotted in Figure 7 as a function of foaming temperature. We can see that over the range of foaming temperatures explored, the average cell diameter remains fairly constant. This behavior is counter intuitive to what we would expect; as the foaming temperature goes up, the polymer viscosity decreases, allowing the cells to grow larger. However, cell growth must compete with cell nucleation for the available gas. From Figure 5, we know that the cell density is increasing exponentially with foaming temperature. Thus more cells are being formed at the expense of cell growth.

The foam density is plotted in Figure 8. We can see that density decreases linearly as the foaming temperature is increased, from 55 °C to 90 °C. This decrease in density is consistent with an increasing cell density and the relatively constant cell diameter across the foaming temperatures explored. Beyond 90°C, The foam density goes through a minimum at approximately 105 °C, and then begins to increase. It appears that above 105 °C the diffusivity of CO_2 has increased to a point where the gas diffuses out of the sample instead of supporting cell nucleation and growth. From Figure 8 we can also see that the relative density has dropped to approximately 0.15 at 105 °C, an 85% reduction in the density of the original PVC.

3.3 RATE OF CELL GROWTH

The rate of cell growth is an important process parameter. The cell growth rate is a complex function of the viscosity and surface tension of the polymer, and the solubility and diffusivity of the gas within the matrix. To determine the rate of cell growth in the PVC - CO_2 system, samples were foamed at 75 °C for increasing foaming times, ranging from 10 seconds, to a maximum foaming time of 4 minutes. The foaming temperature of 75 °C was chosen based on the previous experiment, corresponding to a relative density of 50%, for 30 seconds of foaming time, as shown in Figure 8. Figure 9 shows microcellular PVC samples foamed at increasing foaming times. Again, to facilitate a visual comparison, all micrographs in Figure 9 were taken a constant magnification of 350X. We can see that initially (micrograph a) that the cell density is quite high, and rapidly drops as the foaming time is increased (micrograph d). We can also see from Figure 9 that the cells in micrographs a,b, and c are subsequently larger, and from micrograph d onward, the average cell size remains fairly constant. The average cell diameter is plotted in Figure 9 as a function of the foaming time. We can see that the average cell size grows rapidly in the first 50 seconds and then reaches a limiting value of approximately 18 μm after the driving force for growth has been depleted. The cell density as a function of the foaming time is plotted in Figure 11. We can see that the cell density drops by an order of magnitude within the first 50 seconds of growth due to bubble coalescence. The cell density and average cell diameter determine the void fraction, and thus the density of the foam. The relative density is plotted as a function of foaming time in Figure 12. We can see that the relative density approaches a limiting value after approximately 100 seconds, which is consistent with the data shown in Figures 10 and 11. We note also that for a foaming time of 30 seconds in this experiment, a foam relative density of 0.49 is obtained, which is consistent with the data in Figure 8.

4.0 CONCLUSIONS

We have presented details of a process to produce microcellular PVC foams with a wide range of foam relative densities. In this study, foam relative densities obtained ranged from 0.15 to 0.94. The following conclusions can be drawn regarding the PVC - CO_2 system:

1. Bubble nucleation and growth can occur at temperatures well below the glass transition temperature of the original polymer. The lowest temperature at which a significant bubble growth occurred was found to be 55 °C for PVC saturated with 4.8 MPa carbon dioxide.
2. Over the temperature range of 55 - 120 °C, the bubble nucleation density appears to increase exponentially, showing an Arrhenius - type dependence on temperature. The average bubble diameter was found to be relatively constant with temperature.
3. The density of microcellular PVC decreases monotonically with temperature in the range of 55 °C to 105 °C. Therefore, accurate control of the foam density is possible by controlling the foaming temperature.
4. Much of the cell growth takes place within the first 60 seconds of foaming. Beyond this time, the foam structure does not appear to change significantly. A foaming time of 20 to 30 seconds is adequate to obtain bubbles of approximately 10 μm in diameter.

4.1 FUTURE RESEARCH

We believe that the discovery of microcellular PVC has the potential to significantly impact the vinyl industry. Microcellular PVC with relative densities in the 0.7 to 0.9 range may be able to replace solid PVC now used in a number of applications, offering significant reduction in materials costs. In lower relative density ranges, microcellular PVC is expected to offer a new range of properties to the engineer due to its extremely homogeneous microstructure.

Our research plans call for continued investigation of the key process parameters, particularly the effect of gas saturation pressure on the resulting microstructure. In the next phase of the program we plan to measure the mechanical properties of these novel materials.

5.0 ACKNOWLEDGMENTS

We would like to thank Paula Dunnigan of the BFGoodrich Company's GeonVinyl Division in Cleveland, Ohio, for furnishing the PVC samples used in this study. This research was primarily supported by the National Science Foundation Grants DDM 8909104 and MSS 9114840. Partial support was received from the Manufacturing Systems Technology Center of the Washington Technology Centers. This support is gratefully acknowledged. Thanks also to University of Washington undergraduate students Brian Lee, Robert Lee, and Micki Nguyen for assisting in some of the experiments reported in this paper.

6.0 REFERENCES

1. Personal communication with Professor Nam P. Suh of MIT.
2. Martini, J.E., Suh, N.P., and Waldman, F.A., US Patent No. 4,473,665, 1984.
3. Kumar, V., and Suh, N.P., "A Process for Making Microcellular Thermoplastic Parts," *Poly. Eng. & Sci.*, Vol. 30, No. 20, Oct. 1990, pp. 1323-1329.
4. Kumar, V., "Process-Synthesis for Manufacturing Microcellular Thermoplastic Parts," Ph.D. Thesis, Department of Mechanical Engineering, MIT, 1988.
5. Colton, J., and Suh, N.P., "Nucleation of Microcellular Foam with Additives: Part I: Theoretical Considerations," *Poly. Eng. and Sci.*, Vol. 27, No. 7, pp. 493-499, 1987.
6. Colton, J., and Suh, N.P., "Nucleation of Microcellular Foam with Additives: Part II: Experimental Results," *Poly. Eng. and Sci.*, Vol. 27, No. 7, pp. 485-492, 1987.

7. Kweeder, J. A., Ramesh, N. S., Campbell, G. A., and Rasmussen, D. H., "The Nucleation of Microcellular Polystyrene Foam," *SPE Technical Papers*, Vol. XXXVII, pp. 1398-1400.

8. Ramesh, N. S., Dontula, D., Rasmussen, D., and Campbell, G. A., "Theoretical and Experimental Study of the Dynamics of Foam Growth in Thermoplastic Materials," *SPE Technical Papers*, Vol. XXXVII, pp. 11292-1296.

9. Kumar, V., and Weller, J. E. "Microcellular Polycarbonate Part I: Experiments in Bubble Nucleation and Growth," *SPE Technical Papers*, Vol. XXXVII, pp. 1401 - 1405.

10. Kumar, V., and VanderWel, M., "Microcellular Polycarbonate Part II: Characterization of Tensile Modulus," *SPE Technical Papers*, Vol. XXXVII, pp. 1406 - 1410.

11. Kumar, V., Weller, J. E., and Hoffer, H. Y., "Synthesis of Microcellular Polycarbonate: A Phenomenological Study of Bubble Nucleation and Growth," *Symposium on Processing of Polymers and Polymeric Composites*, ASME Winter Annual Meeting, Dallas, Nov. 1990, Vol. MD-19, pp. 197-212.

12. Berens, A. R., "Solubility and Diffusion of Small Molecules in PVC," *SPE Technical Papers*, Vol. XXXV, pp. 722 - 724.

13. Tikhomirov, B. P., Hopfenberg, H. B., Stannett, V. T., and Williams, J. L., *Makromol. Chem*, Vol. 118, 177, 1968.

14. Kumar, V., and Weller, J. E. "Creating an Integral, Unfoamed Skin on microcellular Foams," to be presented at the Symposium on Microcellular Foams at the Society of Plastics Engineers Annual Technical Conference in Detroit, May 1992.

15. Shutov, F. A., Integral Structural Polymer Foams, Springer - Verlag, New York, 1986.

16. Chow, T. S., *Macromolecules*, Vol. 13, p. 362, 1980.

17. Chiou, J. S., Barlow, J. W., and Paul, D. R., "Plasticization of Glassy Polymers by CO_2," *J. Appl. Poly. Sci.*, Vol. 30, pp. 2633-2642, 1985.

18. Crank, J., The Mathematics of Diffusion, 2nd Edition, Oxford Science Press, New York, 1989.

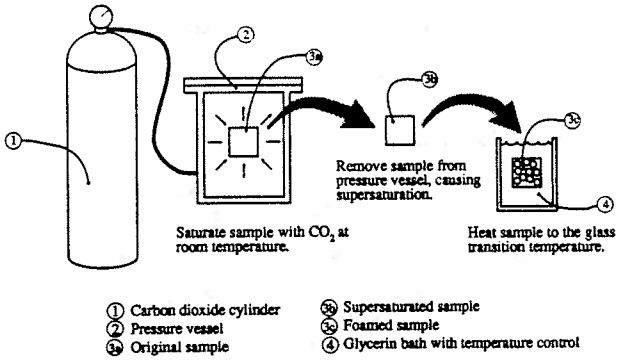

Figure 1. Schematic of the process to produce microcellular PVC.

Appendix A - Diffusivity of Carbon Dioxide in PVC

The diffusivity of carbon dioxide in PVC was measured in a desorption experiment. A PVC sample, 2.05 mm thick, was saturated with CO_2 maintained at 4.8 MPa (700 psi) and 20 °C . The samples were then withdrawn from the pressure vessel and weighed periodically until the amount of carbon dioxide remaining in the samples was approximately 80 percent of the equilibrium value at saturation. For early states of diffusion of gas from the disks, the amount of gas remaining in the disk at any time is related to the diffusion coefficient $\mathcal{D}$ by [18]

$$\frac{M_t}{M_\infty} = 1 - \frac{4}{\sqrt{\pi}}\left(\frac{\mathcal{D}\,t}{\ell^2}\right), \qquad \text{(A1)}$$

where

M_t = amount of gas remaining in the polymer at time t, g,
M_∞ = amount of gas at equilibrium saturation, g,
$\mathcal{D}$ = diffusion coefficient, cm^2/sec,
ℓ = sample thickness, cm,
t = elapsed time in seconds.

If $\frac{M_t}{M_\infty}$ is plotted against $\sqrt{t/\ell^2}$, then the slope R is given by

$$R = \frac{4\sqrt{\mathcal{D}}}{\sqrt{\pi}}, \qquad \text{(A2)}$$

and the diffusion coefficient can be found from

$$\mathcal{D} = \frac{\pi R^2}{16}. \qquad \text{(A3)}$$

Figure A1 shows a plot of $\frac{M_t}{M_\infty}$ as a function of $\sqrt{t/\ell^2}$ for our desorption experiments. From this data an average diffusion coefficient for carbon dioxide-polycarbonate system was determined to be 1.3×10^{-8} cm^2/sec.

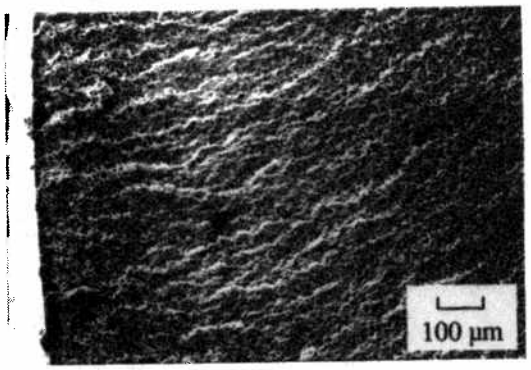

Figure 2. Scanning electron micrograph of microcellular PVC, showing a homogeneous structure across the thickness.

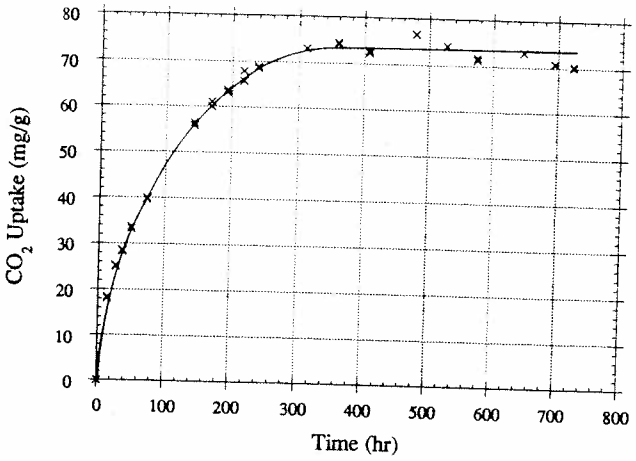

Figure 3. Sorption curve for PVC in CO_2 at 700 psi and 20 °C.

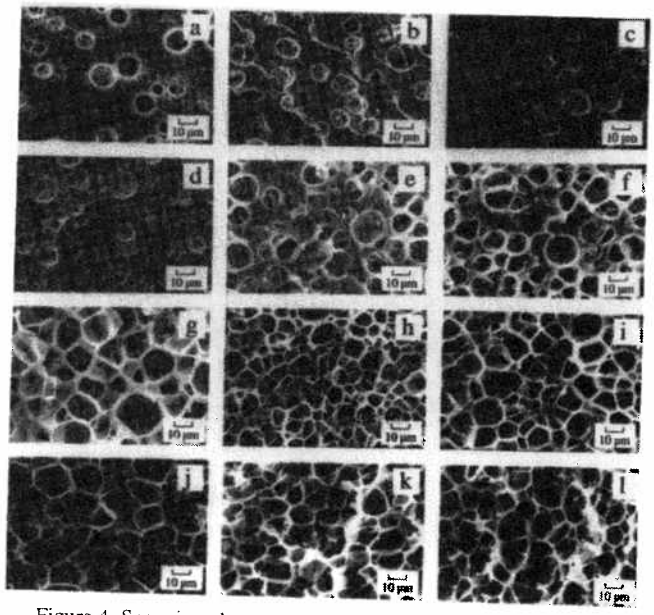

Figure 4. Scanning electron micrographs of microcellular PVC foamed at different temperatures: a(56°C), b(61°C), c(65°C), d(70°C), e(75°C), f(80°C), g(90°C), h(95°C), i(100°C), j(105°C), k(110°C), l(115°C).

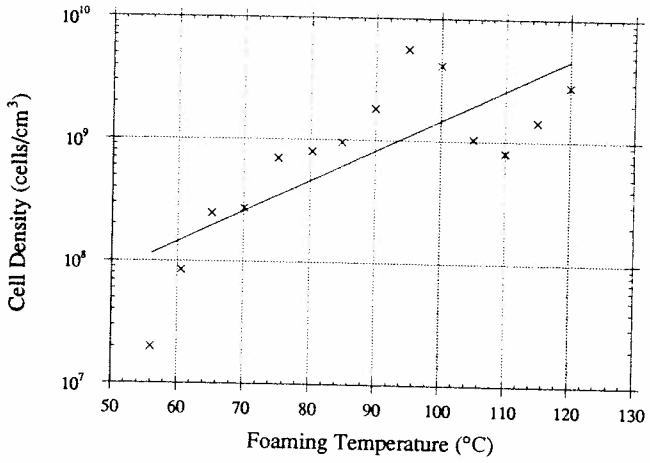

Figure 5. Plot of cell density as a function of foaming temperature.

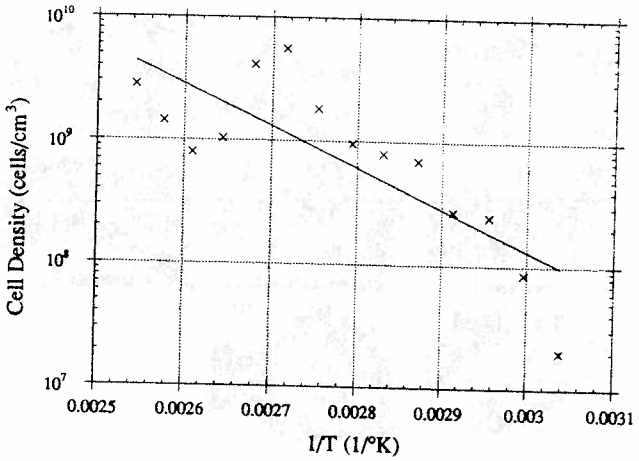

Figure 6. Plot of cell density as a function of inverse absolute temperature.

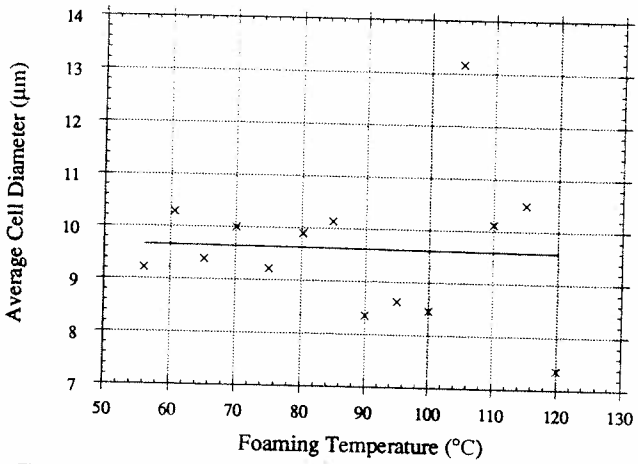

Figure 7. Plot of average cell diameter as a function of foaming temperature.

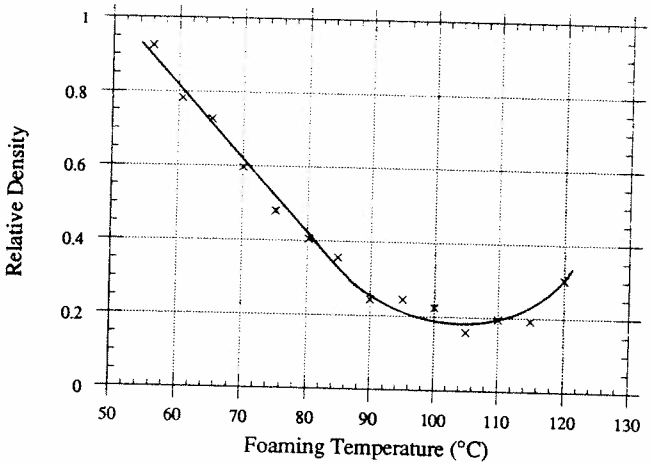

Figure 8. Plot of foam relative density as a function of foaming temperature.

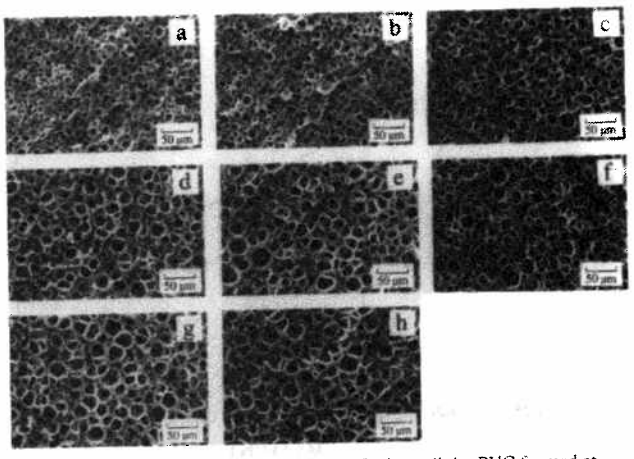

Figure 9. Scanning electron micrographs of microcellular PVC foamed at different times: a(10 sec), b(20 sec), c(30 sec), d(40 sec), e(60 sec), f(90 sec), g(120 sec), h(240 sec).

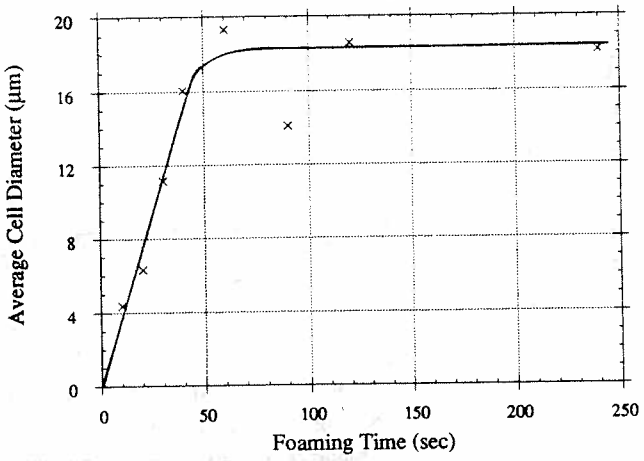

Figure 10. Plot of average cell diameter as a function of foaming time.

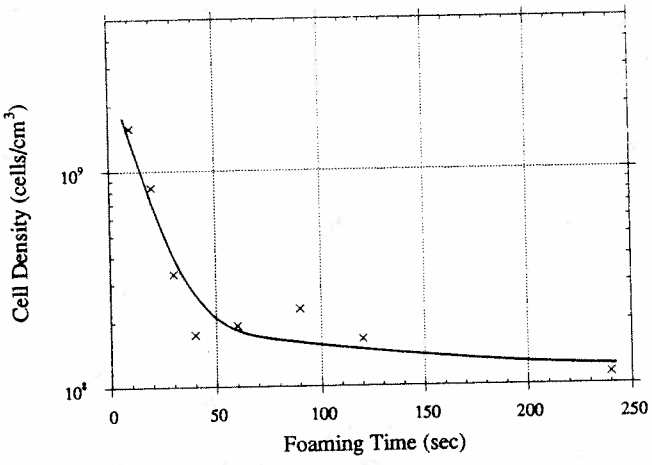

Figure 11. Plot of cell density as a function of foaming time.

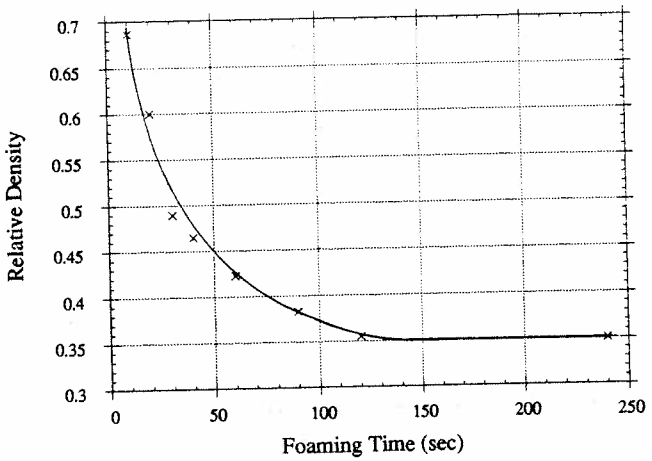

Figure 12. Plot of relative foam density as a function of foaming time.

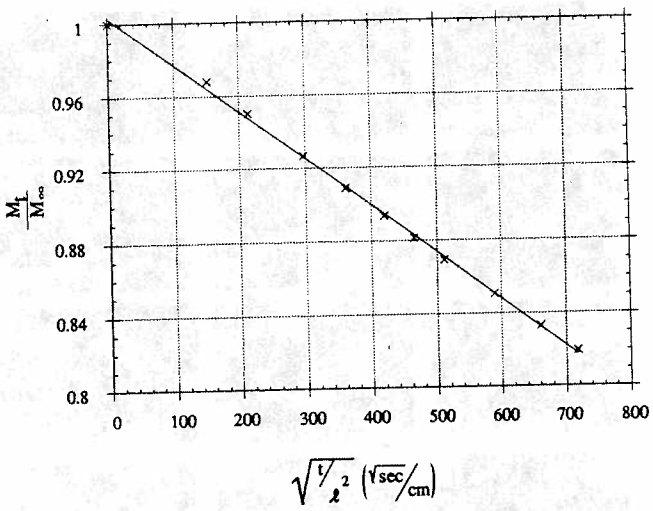

Figure A1. Desorption plot for the PVC - carbon dioxide system.